I&EC research
Industrial & Engineering Chemistry Research
pubs.acs.org/IECR
Article

Graphene Oxide Synthesis: Reaction Calorimetry and Safety

Pritishma Lakhe, Devon L. Kulhanek, Xiaofei Zhao, Maria I. Papadaki, Mainak Majumder, and Micah J. Green*

Cite This: *Ind. Eng. Chem. Res.* 2020, 59, 9004−9014
Read Online
ACCESS | Metrics & More | Article Recommendations | Supporting Information

ABSTRACT: While several studies have been published to optimize the oxidation−exfoliation process of modified Hummers' method to make graphite oxide (GO), relatively few studies have explored the effects of operating conditions on the final GO product or process safety concerns with the GO synthesis process. In this study, reaction calorimetry is used to determine the heat of solution and oxidation reaction for a modified Hummers' method as a function of reactor processing parameters. We find that the heat of reaction increases when graphite is soaked in sulfuric acid for an extended time compared to an oxidation process without extended soaking of graphite in acid. GO synthesized with acid-soaked parent material has more surface functional groups, and the heat of the oxidation reaction decreases with increasing stirring rate. In contrast, GO synthesized with non-acid-soaked parent material has more edge functionalized groups and the heat of reaction does not vary with stirring speed. The study shows the heats of solution and reaction are high enough to reach the reported unstable temperature of Mn_2O_7; however, the amount of Mn_2O_7 generated in a typical modified Hummers' method is dilute enough to avoid a violent reaction at 55 °C.

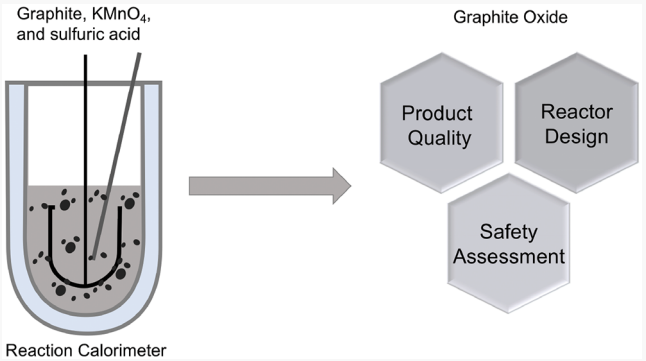

1. INTRODUCTION

Since it was first isolated as a two-dimensional atomic monolayer in 2004, graphene has revealed a broad array of valuable applications ranging from electronic devices to pharmaceuticals to structural reinforcement to catalysis.[1−6] Industrial interest in large-scale production of graphene has rapidly increased as these applications approach commercial feasibility.[7] While bottom-up synthesis procedures such as chemical vapor deposition result in a pristine, high-quality graphene, they have extremely low yield and are difficult to scale up to meet the demand.[8] Alternatively, top-down procedures involving the chemical synthesis of graphite oxide (GO) from graphite are being considered for their high yield and scalability, despite resulting in sheets with more defects.[9] In the chemical synthesis approach, graphite is initially converted to graphite oxide before being exfoliated into single-layer graphene oxide. The graphene oxide may then be reduced either chemically or thermally to remove oxygen functional groups and form a graphene-like material, termed reduced graphene oxide (rGO).[10,11]

The oxidation of graphite occurs in three stages: (1) formation of graphite intercalated compound (GIC) in the presence of strong acid, (2) oxidation of GIC by strong oxidizer, and (3) termination of oxidation reaction by water addition.[12] The addition of H_2O_2 after water addition dissolves the Mn species, assisting in GO purification.[13,14] Many synthetic routes for producing GO have been developed which vary the strong acid solvent, the strong oxidizing reagent, and the relative quantities of each component.[15−18] Hummers' method, as well as its modified versions, are widely used synthetic routes for GO production. The methods have evolved over time to utilize more practical materials and procedures. Today, modified versions of Hummers' method, which uses concentrated sulfuric acid as the acid solvent and a combination of $NaNO_3$ and $KMnO_4$ as the strong oxidizer, are some of the most widely used procedures for GO synthesis.

Numerous studies have been conducted to improve on the original Hummers' method. Morimoto et al. examined each step of the modified Hummers' method to optimize the oxidation process and eliminate steps that do not positively affect oxidation.[13] They summarized that the optimal conditions to synthesize GO were to react $KMnO_4$ and graphite at a ratio of 3:1 in sulfuric acid at a reaction temperature of 35 °C for 2 h, followed by water and hydrogen peroxide addition, respectively. Lavin-Lopez et al. have optimized the modified Hummers' method to make the process scalable and economic.[19] Dimiev et al. concluded that

Received: February 8, 2020
Revised: April 21, 2020
Accepted: April 22, 2020
Published: April 22, 2020

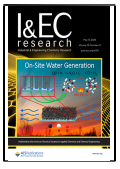

https://dx.doi.org/10.1021/acs.iecr.0c00644
Ind. Eng. Chem. Res. 2020, 59, 9004−9014

the oxidation reaction is diffusion-controlled and dependent on the graphite grain size.[12] Seiler et al. further reported that the degree of intercalation of graphite by the acid determines the degree of oxidation of graphite and that intercalation can happen in a matter of minutes.[12,20,21] The authors further noted that the oxidation reaction does not occur at low temperatures (<20 °C) and high temperature (>35 °C) oxidation leads to the formation of defects in GO.[13,22] In order to reflect an optimized Hummers' method likely to be used in GO production, we focus on the case of 3:1 $KMnO_4$ to graphite ratio in sulfuric acid and at a reaction temperature of 35 °C for 2 h.

While several studies have been published to optimize the oxidation−exfoliation process,[13,14] relatively few studies have explored the effect of operating conditions on the heat of reaction and the final GO produced. Lee et al. reported the heat of solution for $KMnO_4$ in sulfuric acid, and the reaction for graphite oxidation.[23] They reported a higher heat of solution compared to the heat of reaction and concluded that controlling the heat released is more important during the $KMnO_4$ addition step than during the oxidation reaction step.[23] In principle, the heat of reaction and solution should not vary with operating parameters such as reaction temperatures and stirring rate. However, if a difference is detected in these quantities due to change in operating conditions, it indicates that the operating conditions are affecting the reaction kinetics.

The heat of reaction can indicate the characteristics of the final GO product (degree of oxidation and functionalization), as well as the related safety considerations for modified Hummers' method. A greater understanding of the risks associated with the production of GO, such as thermal management and chemical stability, will be increasingly important as the process is brought to an industrial scale. Prior studies have pointed out the importance of controlling the heat released by $KMnO_4$ addition and oxidation reaction[13,23] because dissolution of $KMnO_4$ in acid produces dimanganese heptaoxide, Mn_2O_7, which is considered unstable at elevated temperatures of 55 °C and sensitive to organic impurities.[24,25]

Here, we evaluate the oxidation reaction from a reaction engineering perspective to address potential safety issues in scaling up this process. Our focus is the heat release rate at the oxidation step. The heat release rate is quantified using a heat flow reaction calorimeter. The effects of operating conditions such as reaction temperature, acid treatment time, and stirring rate are investigated and their influence on the heat of reaction and the final final GO product are studied. Finally, the thermal hazards of Mn_2O_7 are studied in a pseudoadiabatic calorimeter at the operating conditions of modified Hummers' method.

2. METHODOLOGY

2.1. Materials. Graphite powder with an average particle size of 81 μm was obtained from Bay Carbon, Inc. Potassium permanganate ($KMnO_4$), hydrogen peroxide (H_2O_2), 37 wt % hydrochloric acid (HCl), and 95 wt % sulfuric acid (H_2SO_4) were procured from Sigma-Aldrich, and their product codes are 223468, 216763, 320331, and 258105, respectively. All the materials were used as received without further purification or treatment.

2.2. Reaction Calorimeter. The oxidation reaction was carried out in a Mettler Toledo Reaction Calorimeter (RC1*e*). The calorimeter features a 1.2 L glass reaction vessel with an anchor impeller and Hastelloy thermocouple. The temperature of the reactor is maintained by a heating/cooling jacket filled with silicon oil which runs through a Jubalo recirculating chiller. With the use of data from vertical and horizontal heat flux sensors on the reactor wall, the temperature was actively controlled by an RTCal thermostat, and the energy released by the reaction was captured by the iControl software in real time. The schematic of the calorimeter is shown in Figure 1.

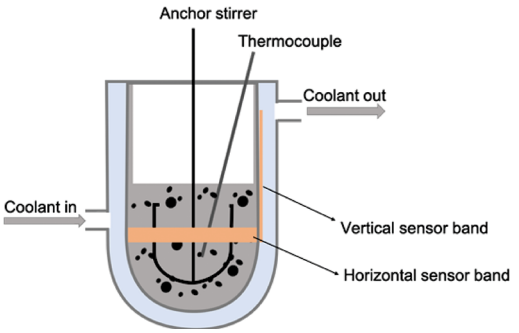

Figure 1. Schematic of reaction calorimeter.

2.3. Experimental Procedure. Graphite oxide was prepared using a modified Hummers' method without pretreatment of the graphite.[16] A 3 g sample of graphite is added to a reactor with 250 mL of 95 wt % sulfuric acid. The reactor temperature is held constant at 10 °C. A 9 g sample of potassium permanganate is added slowly to the reactor, while the reactor temperature is maintained at 10 °C. After permanganate addition, the reactor is heated to 33 °C and held at this temperature for 2 h with stirring. The reactor is then cooled to room temperature, and the reaction mixture is transferred into a flask. The oxidation reaction is terminated by the addition of water to the mixture, followed by hydrogen peroxide addition.

The graphite oxide solution is washed with approximately 2100 mL of 10 wt % HCl to remove salt byproducts.[26] HCl (37 wt %) is mixed with distilled water to create the washing acid. The acid-washed solution is further washed with distilled water until the pH is neutral at 4.5. The sample is either dried under vacuum in an oven at 40 °C for 24 h or flash-frozen in liquid nitrogen and freeze-dried (Vitris Benchtop Freeze-Dryer) for approximately 72 h to yield a dry GO powder.

Here the term "acid-soaked" refers to experiments or GO produced where the parent graphite material was stirred in sulfuric acid for 70 min before $KMnO_4$ was added, whereas "non-acid-soaked" refers to experiments or GO produced where the parent graphite material was stirred in sulfuric acid for less than 10 min. Every experiment was run with the same quantities of graphite, oxidizer, and solvent.

2.4. Characterization Methods. *2.4.1. Thermogravimetric Analysis.* The mass loss due to GO decomposition were measured using a Q50 thermogravimetric analyzer (TGA) from TA Instruments, New Castle, DE. The measurements were made in a nitrogen environment. The sample was heated from room temperature at 1 °C/min to 30 °C. After holding isothermal for 10 min, the samples were heated to 750 °C at a constant rate of 4 °C/min.

2.4.2. XPS. X-ray photoelectrron spectroscopy (XPS) measurements were conducted using Omnicron XPS. Deconvolution of XPS C 1s spectra was done using CasaXPS software using Shirley type background.

https://dx.doi.org/10.1021/acs.iecr.0c00644
Ind. Eng. Chem. Res. 2020, 59, 9004−9014

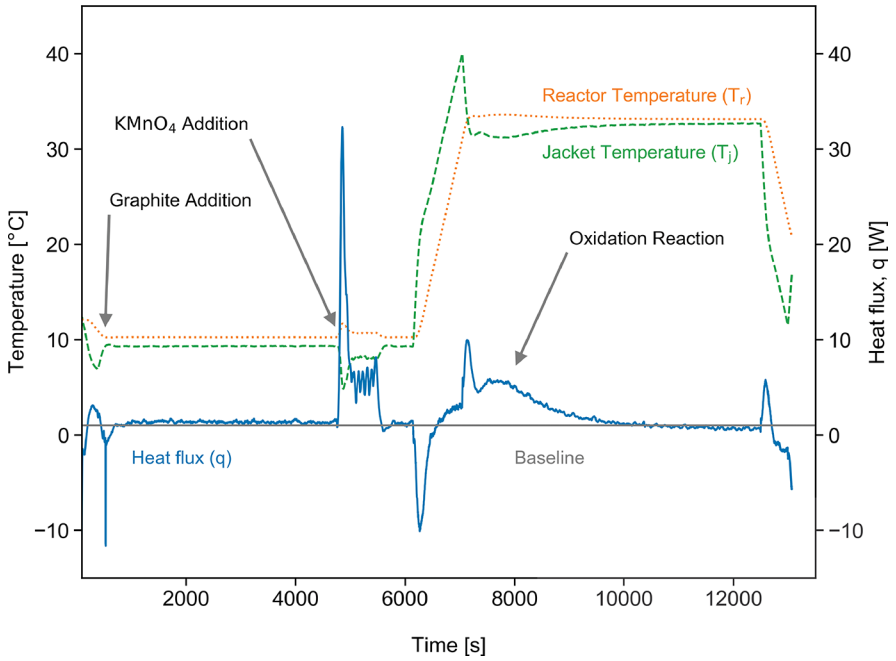

Figure 2. Data obtained from the RC1*e* reactor. The orange line represents the reactor temperature (T_r), the green line represents the jacket temperature (T_j), and the blue line represents the heat released by the reaction, the heat flux (q). The baseline is the heat released curve when no reaction is happening in the reactor. In order to calculate the heat of dissolution or reaction, the heat flux curve (q) is integrated over time from when it gets higher than the baseline and until q recovers back to the baseline.

2.4.3. Elemental Analysis. Via a third-party testing service, CHN and direct oxygen analysis were conducted according to the ASTM D-5291 standard using a PE 2400 CHN analyzer fitted with an oxygen accessory kit.

2.5. Thermal Analysis of Sulfuric Acid and Potassium Permanganate. Analysis of the thermal stability of Mn_2O_7 produced as a result of mixing sulfuric acid and $KMnO_4$ was conducted in the Advanced Reactive System Screening Tool (ARSST) manufactured by Fauske and Associates, Burr Ridge, IL. The ARSST is an open test cell capable of handling chemical systems for temperatures as high as 500 °C and pressures up to 500 psig. The acid and $KMnO_4$ samples were heated at a constant rate of approximately 1.2 °C/min. The sample cell was a glass test cell with a volume of 10 mL, which was placed inside a 350 mL stainless-steel vessel. A thermocouple and pressure transducer tracked the dynamic temperature and pressure changes during the decomposition process. The pressure transducer is located outside the glass test cell in the 350 mL vessel; the thermocouple touched the sample mass.

3. RESULTS AND DISCUSSION

3.1. Heat of Solution. In Figure 2, representative plots of the reactor temperature (orange), jacket temperature (green), and heat flux from the reactor (blue) during the reactor operation in an RC1*e* are shown. The heat flux shows distinct thermal events that occur during the experimental procedure. Prior to t = 0, the reactor was held isothermally at 10 °C and contained 250 mL of 95 wt % H_2SO_4; then, five distinct events can be seen in the heat flux curve:

1. Just after t = 250 s, 3 g of graphite is added to the acid solution and brought from room temperature to 10 °C.
2. At 4200 s, 9 g of $KMnO_4$ is added in 1 g increments and appears as a set of nine exothermic peaks.
3. At 6000 s, the set point of the reactor is increased to the reaction temperature of 33 °C; hence an endothermic peak appears as the reaction mixture is heated.
4. Immediately after heating, a broad exothermic peak corresponds to the heat of reaction between $KMnO_4$ and graphite.
5. Finally, an endotherm appears when the product mixture is rapidly cooled back to room temperature at 12 000 s.

The total heat released or absorbed by the reactor for a given time can be computed by numerical integration of the heat flow rate over that period, i.e.

$$\Delta H = \int_{t_i}^{t_f} q_r \, dt \tag{1}$$

where initial (t_i) and final (t_f) reaction times and the baseline of heat flux are manually selected. The baseline (gray line in Figure 2) shows the overall heat flux when no reaction was occurring in the reactor.

Adding an increment of $KMnO_4$ to the reactor causes the heat flux to rapidly increase, and as $KMnO_4$ dissolves, the heat flux returns to baseline. $KMnO_4$ was manually added to the reactor in 1 g aliquots. A total of 9 g of $KMnO_4$ was added, which is seen in the $KMnO_4$ addition in Figure 2. The heat of solution of $KMnO_4$ in sulfuric acid is addition limited because when the first aliquot of the oxidizer is added, the heat flux curve increases and then decreases as the oxidizer dissolves. Similarly, addition of a second aliquot of oxidizer increases the heat flux, which then decreases as $KMnO_4$ dissolves. The $KMnO_4$ addition in Figure 2 shows multiple peaks for multiple aliquots of oxidizer added to the reaction mixture. Therefore, the heat released during this step can be controlled by controlling the feed rate of $KMnO_4$.

Table 1 summarizes the heat of the solution obtained from the reaction calorimeter. When permanganate and sulfuric acid were mixed at 10 °C without graphite, the obtained heat of

https://dx.doi.org/10.1021/acs.iecr.0c00644
Ind. Eng. Chem. Res. 2020, 59, 9004−9014

Table 1. Heat of Solution at 10 °C

condition	heat of solution [kJ/mol $KMnO_4$]	notes	source
$KMnO_4$ and sulfuric acid	79.1	460 g of sulfuric acid	this study
$KMnO_4$, sulfuric acid, and graphite	116.3	460 g of sulfuric acid	
$KMnO_4$ and sulfuric acid	49.1	840 g of sulfuric acid	23

solution was 79.1 kJ/mol $KMnO_4$. This is higher than the previously reported value of an average 49.1 kJ/mol $KMnO_4$ by Lee et al.[23] Lee et al. observed values close to this average at both 10 and 35 °C and with varying permanganate quantities.

Prior literature indicates that oxidation reactions do not occur at 10 °C; however, we noticed a higher heat of solution (an average of 116.3 kJ/mol $KMnO_4$) when permanganate was added to H_2SO_4 that already contained graphite. The higher heat of solution with graphite in the reaction mixture observed here can be attributed to some degree of oxidation reaction even at 10 °C.

3.2. Heat of Reaction. A major consideration in scaling up an exothermic reaction is understanding of the intensity and consequences of the exothermic behavior of the reaction. This information helps in the design of a reactor's cooling capacity to be able to maintain the desired reaction temperature and avoid thermal runaway reactions. In this section, we determined the heat of the oxidation reaction. After the contents of the reactor (graphite, sulfuric acid, and $KMnO_4$) were heated to 33 °C, the heat of reaction appeared in the heat flux curve as a broad, exothermic peak (starting around 6800 s in Figure 2). At this temperature, the reaction is kinetically controlled as seen in Figure 2.

Figure 3a shows the heat of reaction at 33 °C for acid-soaked and non-acid-soaked reactions at three different stirring speeds of 100, 150, and 200 rpm. Each experiment was repeated at least twice, and the straight line is the average value for a given reaction condition. The temperature of the reaction mass was held at 33 °C for 2 h before it was cooled and quenched.

Figure 3b is the C/O molar ratio of the GO products as determined by elemental analysis (EA). The blue line represents the molar ratio of GO produced from parent graphite that was allowed to soak in acid for an extended time, and the green line is the molar ratio of GO produced from non-acid-soaked parent material. The elemental analysis results are tabulated in Table 2. We have added the table with the carbon and oxygen weight percent and corresponding C/O ratio from XPS in Table S1. The C/O ratios from the XPS and the elemental analysis are different because the XPS calculation may be affected by the atmospheric carbon. The elemental analysis is a more accurate representative of the sample composition. The C/O ratio trend from XPS was similar to that obtained from EA although the carbon content is higher in the XPS data.

Table 2. Elemental Analysis Data for GO Synthesized in the RC1*e*

sample (rpm−condition)	C [%]	H [%]	O [%]	C/O molar ratio
100−acid-soaked	42.11	2.36	38.40	1.10
150−acid-soaked	52.54	1.73	41.62	1.26
200−acid-soaked	51.02	1.82	39.20	1.30
100−non-acid-soaked	53.03	1.66	40.12	1.32
150−non-acid-soaked	47.05	2.12	36.44	1.29
200−non-acid-soaked	52.34	1.77	38.91	1.35

Lee et al. previously reported the heat of oxidation reaction for Hummers' method as 126.9 kJ/mol $KMnO_4$ at 1:3 mass ratio of graphite to $KMnO_4$ and reaction temperature of 35 °C. Our data indicated a similar heat of reaction for non-acid-soaked experiments. Non-acid-soaked graphite shows a consistent heat of reaction regardless of rpm with an average of 133 kJ/mol $KMnO_4$ (Figure 3b). This is within the error bar

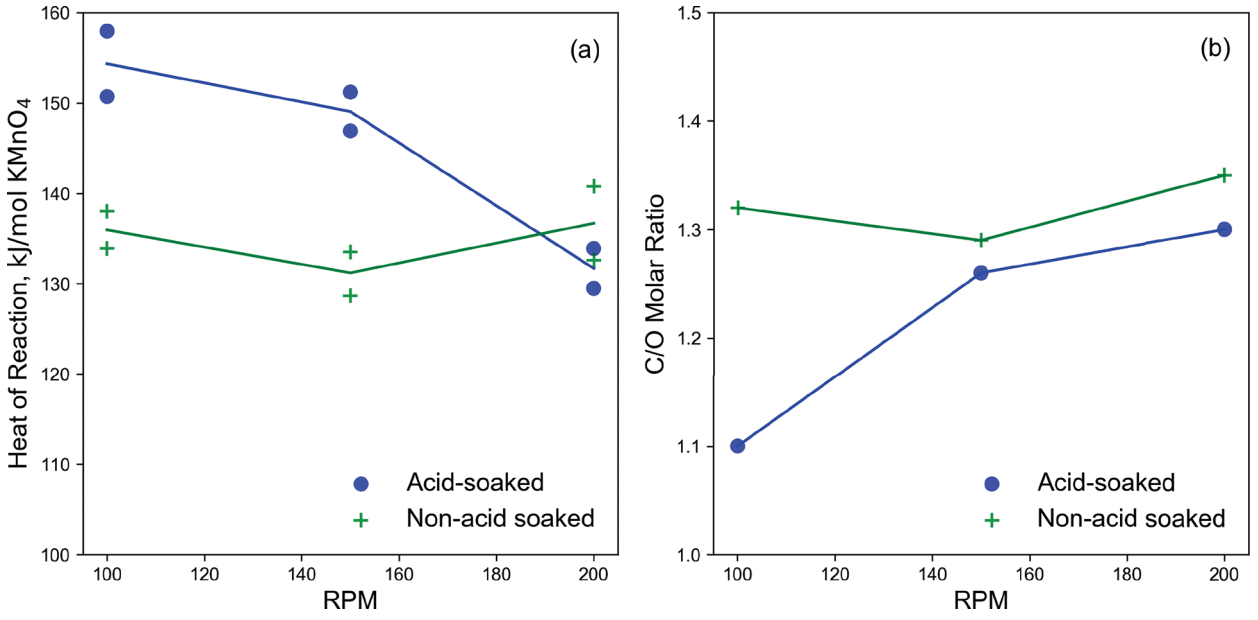

Figure 3. (a) Reported values of heat of oxidation reaction and (b) C/O ratio obtained from elemental analysis with varying agitation (rotation per minute). The blue symbols represent the acid-soaked runs, whereas the green symbols represent the non-acid-soaked runs. The lines represent the average value of the data points.

https://dx.doi.org/10.1021/acs.iecr.0c00644
Ind. Eng. Chem. Res. 2020, 59, 9004−9014

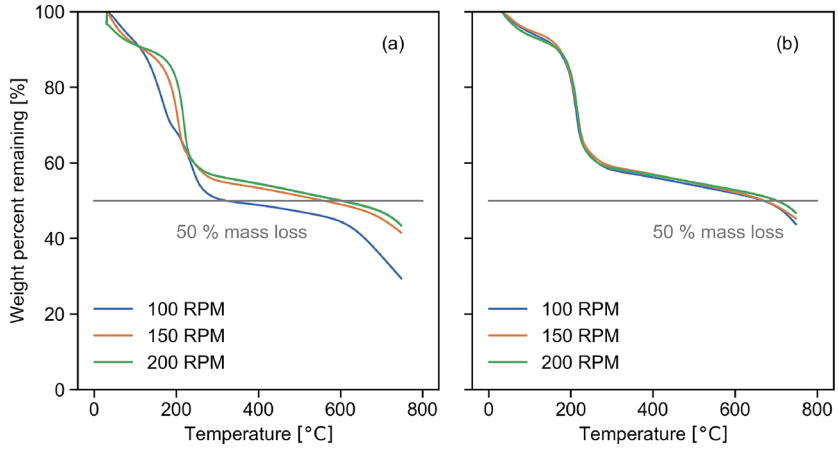

Figure 4. TGA of samples. (a) Decomposition data for acid-soaked samples. A 100 rpm acid-soaked sample decomposes rapidly compared to the 150 and 200 rpm samples. (b) Decomposition data for the non-acid-soaked samples.

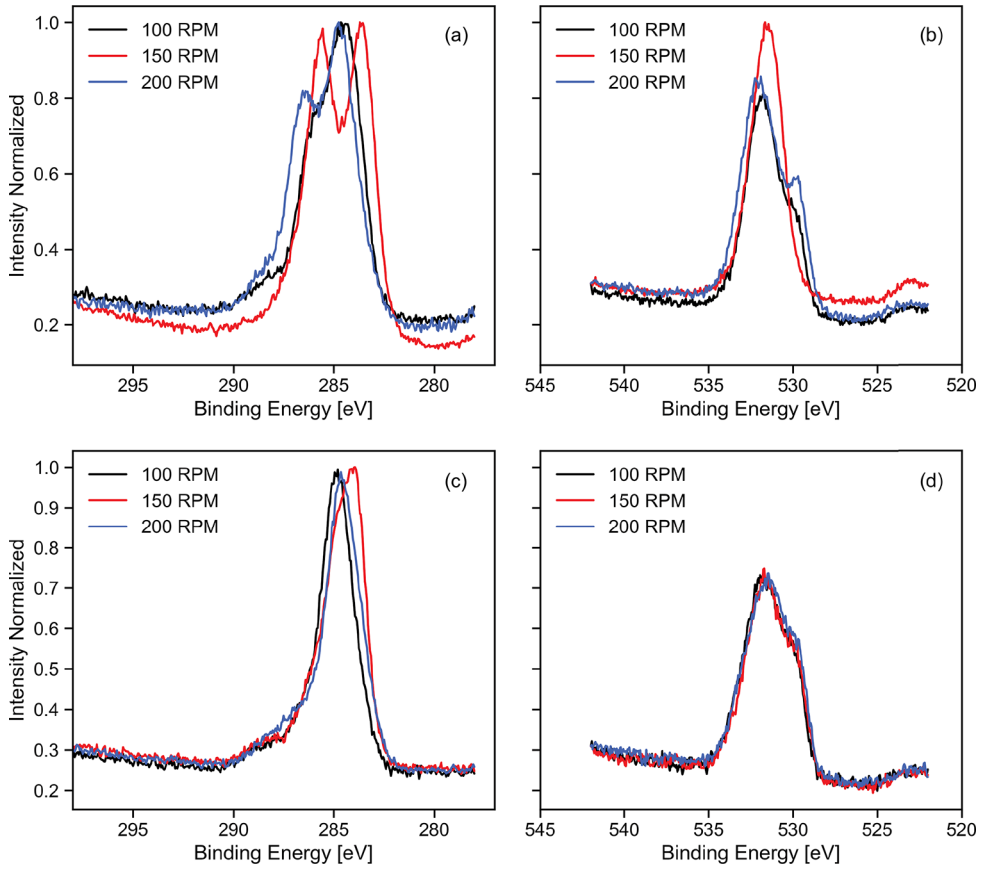

Figure 5. XPS data for GO for different reaction conditions. (a and b) C 1s and O 1s XPS spectra for acid-soaked GO respectively. (c and d) C 1s and O 1s XPS spectra of non-acid-soaked samples. The intercalation increases the amount of functional oxygen group in the sample.

of the data for each rpm tested. The EA of the product GO shows a consistent C/O molar ratio of 1.32 (between 1.29 and 1.35) for non-acid-soaked GO.

For the acid-soaked runs where the graphite parent material is allowed to soak in acid for 70 min before addition of the oxidizer, both the average heat of reaction and the degree of oxidation are higher than for the non-acid-soaked runs. In addition, the heat of reaction and degree of oxidation also vary with the rpm as seen in Figure 3. A lower C/O ratio indicates a higher degree of oxidation and vice versa.

The trends in Figure 3 yield two key observations: (1) acid soaking for an extended time affects the degree of oxidation and (2) for the acid-soaked runs, the rpm affects the degree of oxidation.

To understand these observations, we first examined the TGA data of the final GO produced by acid soaking and non acid soaking of the parent graphite. The TGA data for acid-soaked runs in Figure 4a show different decomposition trends from non-acid-soaked runs in Figure 4b. TGA data from the acid-soaked GO demostrate a decreased mass loss with increasing rpm. The decreased mass loss indicates that the

https://dx.doi.org/10.1021/acs.iecr.0c00644
Ind. Eng. Chem. Res. 2020, 59, 9004−9014

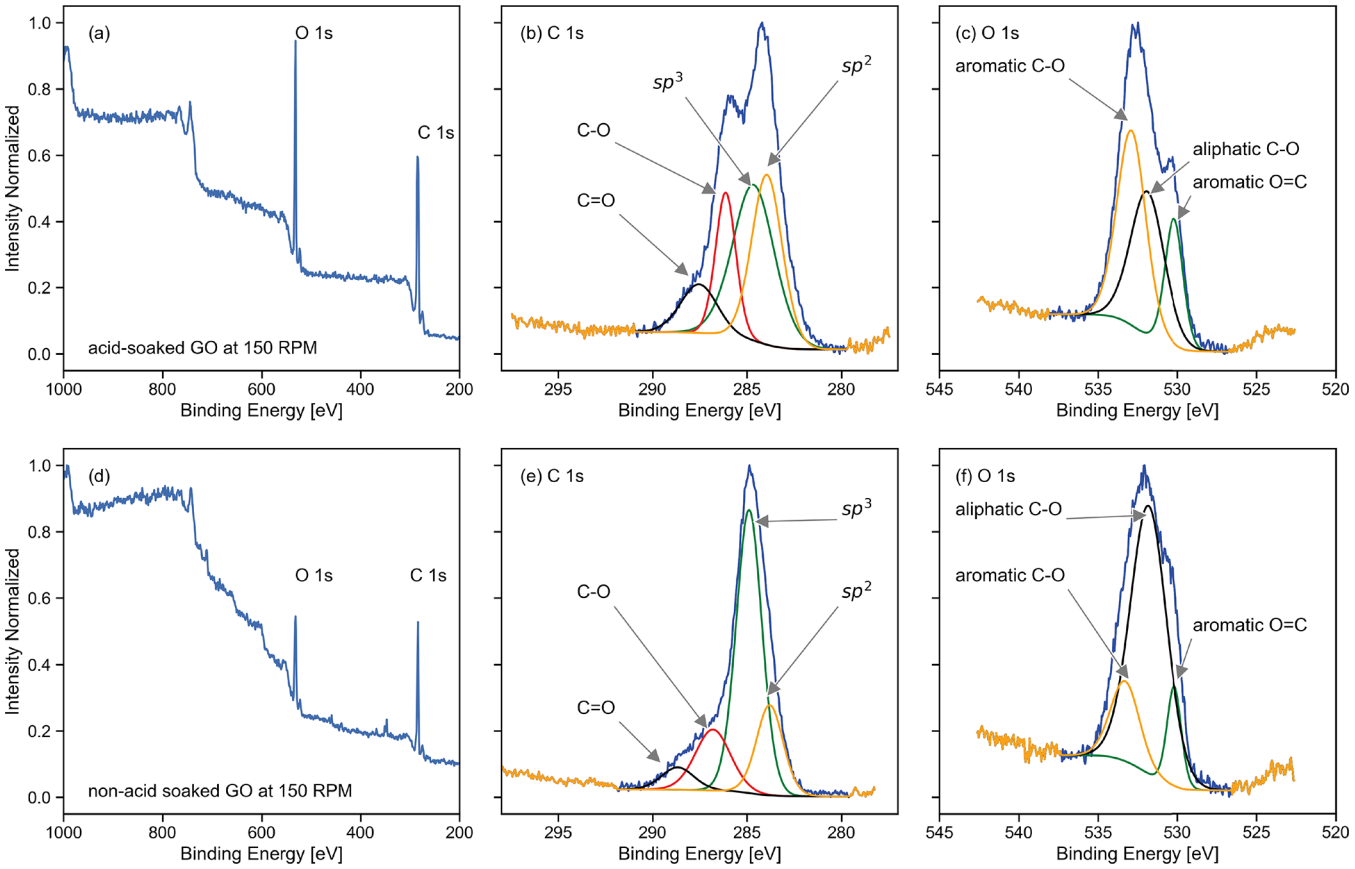

Figure 6. (a) XPS survey of acid-soaked GO, with (b) deconvolution of C 1s peak, and (c) deconvolution of O 1s of acid-soaked peak. (d) XPS survey of non-acid-soaked GO and (e and f) deconvolution of C 1s and O 1s peaks of non-acid-soaked GO, respectively.

sample has fewer oxygen functional groups (Figure 4a). Therefore, 100 rpm acid-soaked GO has the most oxygen groups compared to all other GO synthesis conditions. The TGA trend further aligned with the heat of reaction and EA results. In Figure 3b, the 100 rpm acid-soaked sample has the most oxygen followed by the 150 and 200 rpm samples. In contrast, Figure 4b shows a consistent decomposition trend for all non-acid-soaked samples with different rpm's. Therefore, for non-acid-soaked GO, the degree of oxidation does not change with varying rpm.

In order to understand the first observation, we hypothesize that the extended acid soaking is influencing the degree and type of oxidation occurring in graphite. It is known that intercalation helps with the oxidation of graphite, but prior literature noted that a GIC (graphite intercalated compound) would form in a matter of minutes.[12,21] To our knowledge, there are no studies in the literature investigating the oxygen functionalization of final GO product synthesized by extended soaking of graphite in acid before the addition of $KMnO_4$. However, our results indicate that longer soaking time of parent graphite in acid increases the degree and type of oxidation of graphite.

To investigate the hypothesis that the type of oxidation of graphite is influenced by acid soaking, an XPS analysis was run on the final GO samples. Figure 5 shows the C 1s and O 1s spectra of GO synthesized by acid-soaked and non-acid-soaked graphite in sulfuric acid. The acid-soaked GO has two distinct peaks (Figure 5a) compared to non-acid-soaked GO (Figure 5c) in the C 1s spectra. The O 1s spectra for the acid-soaked GO (Figure 5b) has a more pronounced shoulder compared to the non-acid-soaked GO (Figure 5d).

In this work, we have compared the deconvolution of the XPS spectra of 150 rpm runs for acid-soaked and non-acid-soaked runs. Figure 6 shows that the deconvolution of C 1s spectra for the two sample types indicates far higher sp^3 content in the non-acid-soaked sample. This is surprising because Seiler et al. argued the intercalation of graphite increases the layer distance between the graphite sheets and assists in basal or surface oxidation.[21] The O 1s spectra show that non-acid-soaked GO has significantly more aliphatic C−O compared to the acid-soaked GO as seen in Table 3. This indicates that the functional groups in the non-acid-soaked case are far more concentrated at the nanosheet edges, which does accord with the argument of Seiler et al. We conclude that basal plane functionalization is more prevalent in the acid-soaked case whereas extensive edge functionalization occurs in the non-acid-soaked case. The deconvolution of the O 1s spectra is done using the methods of Vryonis et al.[27]

Table 3. XPS Area Percent for O 1s Subpeak of GO

O 1s subpeak	acid-soaked GO [%]	non-acid-soaked GO [%]
aromatic O=C	18.2	10.8
aliphatic C−O	37.8	72.1
aromatic C−O	43.9	17.1

The corresponding area percent of XPS data is shown in Tables 3 and 4.

https://dx.doi.org/10.1021/acs.iecr.0c00644
Ind. Eng. Chem. Res. 2020, 59, 9004−9014

Table 4. XPS Area Percent for C 1s Subpeak of GO

C 1s subpeak	acid-soaked GO [%]	non-acid-soaked GO [%]
sp^2	31.6	19.2
sp^3	39.8	58.0
C−O	17.8	17.0
C═O	10.8	5.8

The second observation is that for the sulfuric acid soaked graphite, mixing influences the degree of oxidation of the graphite. The heat of oxidation reaction in this paper was calculated by dividing energy released by the reaction by the total moles of $KMnO_4$ added into the system, not the moles of $KMnO_4$ reacted. Therefore, the variation in the heat of reaction could suggest that not all of the $KMnO_4$ added was consumed.

However, the decreasing oxidation (or reaction of $KMnO_4$) with increasing stirring rate is counterintuitive because the increased Reynolds number associated with the stirrer rpm should result in a higher external diffusion rate of $KMnO_4$ to reaction sites between graphite sheets. The Reynolds number (Re) for each rpm is 6500, 9800, and 13 000, respectively (Re calculation is shown in the Supporting Information). At high Re, the convective mass transfer coefficient scales with $Re^{0.5}$ as shown in eq 2.[28]

$$Sh = 2 + 0.6Re^{1/2}Sc^{1/2} \tag{2}$$

where

$$Sh = \frac{k_c d_p}{D_{AB}} \tag{3}$$

$$Re = \frac{\rho d_p v}{\mu} \tag{4}$$

$$Sc = \frac{\nu}{D_{AB}} \tag{5}$$

where Sh is the Sherwood number, Sc is the Schmidt number, k_c is the mass transfer coefficient, d_p is the diameter, D_{AB} is the diffusivity of A in B, ρ is the density, v is the velocity, μ is the viscosity, and ν is the kinematic viscosity. If the reaction is limited by external mass transfer, the rate of reaction (r) is given by eq 6.

$$r = k_c(C_{bulk} - C_{surface}) \tag{6}$$

where C_{bulk} and $C_{surface}$ are concentrations of the oxidation agent in bulk material and surface of the graphite, respectively. Therefore, higher Re gives a higher mass transfer coefficient, k_c, which should improve the diffusion-controlled reaction, given that everything else in the equation is constant. This implies that external mass transfer is not the limiting step in the reaction. Similarly, the trend cannot be attributed to shear-induced particle deagglomeration because higher Re would lead to fewer diffusion limitations and a higher degree of oxidation, which is the opposite of the observed trend.

Other possible physical explanations for this trend include the possibility that increased rpm is promoting a secondary reaction and not the oxidation reaction. Note that running the reactor at very low rpm is inherently unsafe because it slows down the effectiveness of the cooling jacket and allows for local hot spots. Therefore, it is interesting why the oxidation decreases with an increasing stirring rate for acid-soaked samples; this warrants further investigation.

3.3. Reaction Temperature. In this section, the effect of the oxidation reaction temperature on the final GO produced was investigated. Morimoto et al. in their prior work highlighted the need to maintain the temperature of the oxidation reaction at an optimal temperature of 30−35 °C. Their study mentioned that the oxidation reaction at high temperature (i.e., >35 °C) creates defective GO.[13] Therefore, the experiments were conducted for reaction temperatures of 33, 22, and 10 °C.

As we decreased the reaction temperature, the heat of reaction decreased as shown in Table 5. The C/O ratio increased with decreasing temperature, which indicates that less oxygen is present in the final GO. The results from Table 5 indicate that a decrease in oxidation temperature decreases the degree of oxidation. All three experiments were done at 150 rpm and without acid soaking. These experiments were carried out on the samples produced without acid soaking in order to maintain a consistent baseline.

Figure 7a shows the heat flux data for reaction temperatures 10 and 33 °C from the RC1e. Figure 7b is the XPS data of C 1s for GO made at reaction temperatures 10 and 33 °C. The XPS spectra at 10 °C resemble the non-acid-soaked spectra seen at 33 °C.

Figure 8 shows the deconvolution of XPS spectra of GO at two temperatures, 10 and 33 °C, for C 1s and O 1s. Tables 6 and 7 show the area percent of subpeaks. The deconvolution indicates that at higher temperature there are relatively more sp^3 carbon and fewer carbon−oxygen bonds (both C−O and C═O) compared to the GO synthesized at lower temperature. The O 1s spectra indicates that GO at higher temperature has 72.1% aliphatic C−O and GO at lower temperature has 70.1% aromatic carbon and oxygen bonds.

3.4. Mn_2O_7 Hazards in GO Synthesis. In this section, the hazards associated with Mn_2O_7 are investigated. The dissolution of $KMnO_4$ in sulfuric acid is described:[29,30]

$$2KMnO_4 + 2H_2SO_4 \rightarrow Mn_2O_7 + 2KHSO_4 \tag{7}$$

$$Mn_2O_7 + 2H_2SO_4 \rightarrow 2[MnO_3]^+[HSO_4]^- + H_2O \tag{8}$$

The dimanganese heptaoxide, Mn_2O_7, produced by the dissolution of permanganate in sulfuric acid is reported to be unstable.[24,25] Prior literature has noted that temperatures above 55 °C can trigger a violent explosion and/or fire. Mn_2O_7 is sensitive to organic impurities such as acetone, methanol, cotton, etc. and can be explosive at room temperature. The decomposition of Mn_2O_7 is shown in eq 9:[31]

$$4Mn_2O_7 \rightarrow 8MnO_2 + 2nO_3 + (6 - 3n)O_2 \tag{9}$$

Table 5. Heat of Solution and Reaction

reaction temp [°C]	heat of solution [kJ/mol $KMnO_4$]	heat of reaction [kJ/mol $KMnO_4$]	total heat [kJ/mol $KMnO_4$]	adiabatic temp rise [K]	C/O ratio
10	116	9	125	7	N/A
22	113	99	212	15	1.46
33	117	129	246	16	1.29

https://dx.doi.org/10.1021/acs.iecr.0c00644
Ind. Eng. Chem. Res. 2020, 59, 9004−9014

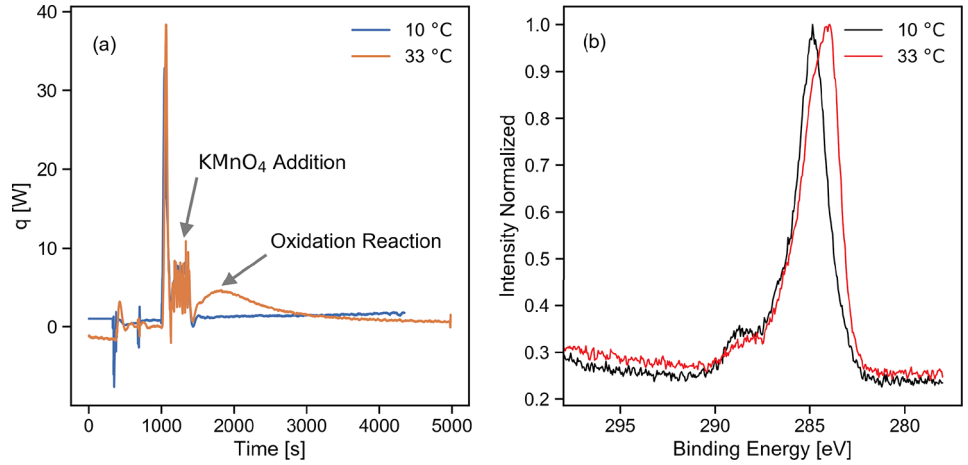

Figure 7. (a) Heat flux data from RC1*e* for reaction temperatures of 33 and 10 °C. (b) XPS C 1s spectra for GO oxidized at temperatures 33 and 10 °C.

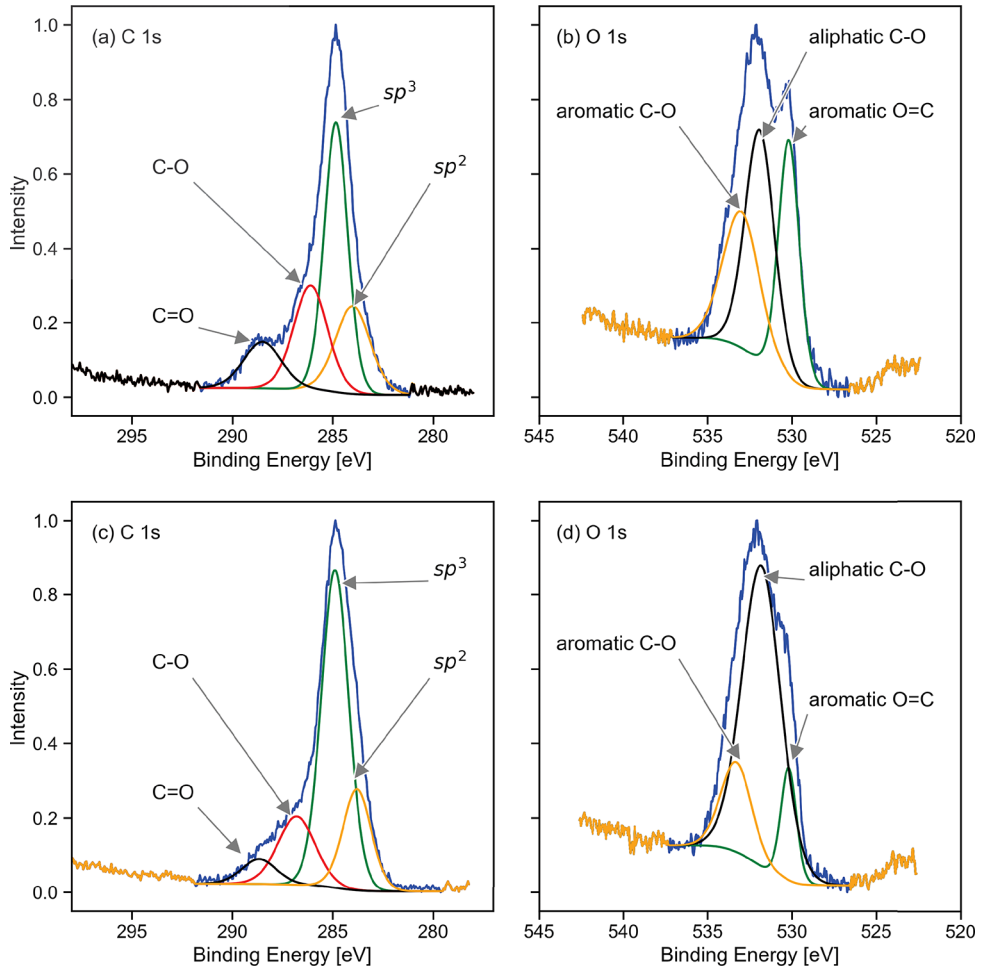

Figure 8. XPS data for GO at different temperatures. (a and b) C 1s and O 1s XPS spectra for non-acid-soaked GO at 10 °C. (c and d) C 1s and O 1s XPS spectra of non-acid-soaked samples at 33 °C.

where $0 < n < 2$. Based on the heats of solution and reaction obtained from the reaction calorimeter in the prior section, the adiabatic temperature increase for the dissolution and oxidation reaction can be up to 16 °C for about 500 g of reaction mass. If the oxidation reaction is performed at 33 °C, the adiabatic temperature increase can be adequate to reach the explosive temperature of 55 °C.

To understand the hazards of Mn_2O_7, we mixed Mn_2O_7 in sulfuric acid at a concentration typically used in modified Hummers' method, 75 mg/mL, and heated to at least 95 °C in the Advanced Reactive System Screening Tool (ARSST). The blue line in Figure 9 is the temperature increase with time, and the red line is the pressure increase with time. A constant heating of 1.2 °C/min was applied for these experiments. If the

https://dx.doi.org/10.1021/acs.iecr.0c00644
Ind. Eng. Chem. Res. 2020, 59, 9004−9014

Table 6. XPS Area Percent for C 1s Subpeak of GO

C 1s subpeak	area percent [%]	
	10 °C	33 °C
sp^2	20.8	19.2
sp^3	43.2	58.0
C−O	24.0	17.0
C═O	12.0	5.8

Table 7. XPS Area Percent for O 1s Subpeak of GO

O 1s subpeak	area percent [%]	
	10 °C	33 °C
aromatic O═C	40.2	10.8
aliphatic C−O	29.9	72.1
aromatic C−O	29.9	17.1

temperature reached at least 95 °C, the external heating was turned off. As seen in Figure 9a, no abrupt increases in temperature or pressure were seen, which indicates that violent decomposition did not occur up to at least 95 °C. Next, we examined the concentrations of permanganate in acid solution commonly used in the literature to see if any of the concentrations are high enough to trigger the self-decomposition of permanganate. Table 8 shows the concentration of oxidizer in acid for modified Hummers' method in various literature sources.

A higher $KMnO_4$ concentration of 150 mg/mL was studied in the reactive screening tool. Even at this concentration, no decomposition was detected as seen in Figure 9b. The temperature and pressure profile increased steadily up to 95 °C, followed by cooling to room temperature. These experiments were carried out in the air, and special care was taken to free the solution of any organic impurities.

Additionally, we examined to see if the addition of graphite in the reaction mixture of sulfuric acid and $KMnO_4$ would trigger the thermal decomposition of the material. Figure 9c shows the thermal data for graphite in 75 mg/mL $KMnO_4$ in sulfuric acid solution. The temperature and pressure profile with time shows a steady increase up to 95 °C and a steady decrease when the heating was turned off. Therefore, no thermal runaway or explosive decomposition was seen.

A further literature review showed that the experiments for the decomposition of dimanganese heptaoxide reported in the literature were done for pure solid Mn_2O_7 in 1953. According to the study, the solid Mn_2O_7 can in fact self-decompose when heated to temperatures above 65 °C and the material is sensitive to shock.[33] Additionally, impurities such as alcohol, acetone, cotton, etc. can ignite concentrated Mn_2O_7 at room temperature.[33] However, in the modified Hummers' method, Mn_2O_7 is in solution and in dilute quantities. Therefore, the hazards of Mn_2O_7 may not be as critical as previously pointed out. Even so, care should be taken to free the reaction mixture of any impurities and avoid isolating or drying the Mn_2O_7 during the process.

Table 8. Permanganate Concentration in Acid Used in Literature

$KMnO_4$ concn [mg/mL]	ref
36.0	this study
26.7	12
120.0	32
60.0	13
20.0−120.0	20

Furthermore, a brief report in 2014 documented at least one safety incident while conducting modified Hummers' method for GO synthesis.[34] In the letter, the authors note that the alcohol (a common reagent in laboratories) reacted with reactants of Hummers' method to synthesize an explosive component. Therefore, to conduct Hummers' method safely, it is crucial that no impurities are present in the reactor and associated equipment.

Another potential safety issue pointed out in prior literature is the possibility of hot spots. The hot spots could become an issue when water is added to the acidic reaction mixture to quench the reaction. The acid and water reaction is extremely exothermic, and the viscosity of the mixture increases with water concentration in the mixture. When the water becomes excess in the mixture, the viscosity decreases. Therefore, it is recommended that the reaction mixture is added to the water and not the other way round.

4. CONCLUSIONS

This study shows that the amount of heat released during the oxidation reaction in the modified Hummers' method corresponds to the degree of oxidation of graphite. Graphite soaked in sulfuric acid for more than an hour before addition

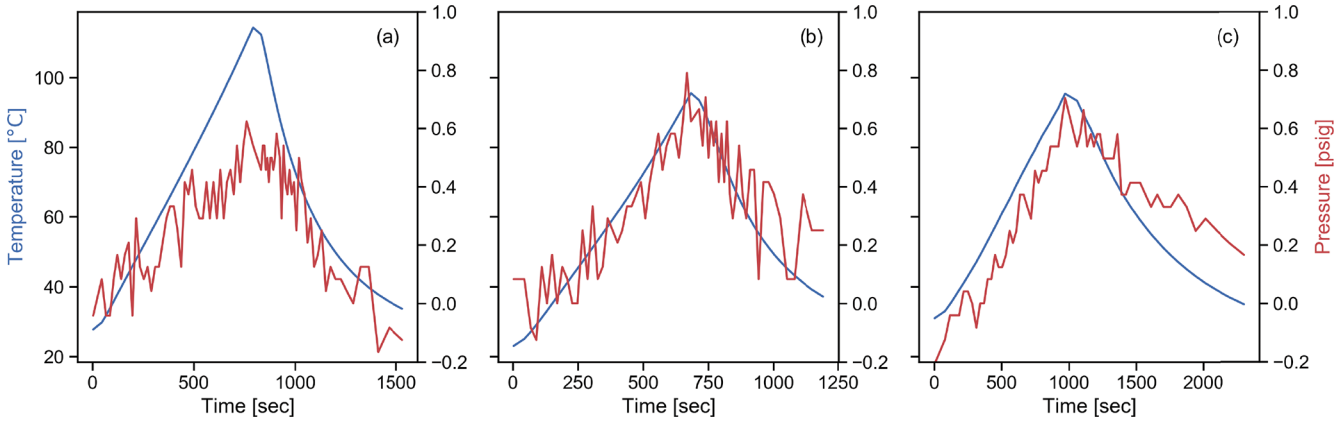

Figure 9. ARSST temperature (blue) and pressure (red) data: (a) 75 mg/mL $KMnO_4$ in H_2SO_4; (b) 150 mg/mL $KMnO_4$ in H_2SO_4; (c) graphite in 75 mg/mL $KMnO_4$ in H_2SO_4.

https://dx.doi.org/10.1021/acs.iecr.0c00644
Ind. Eng. Chem. Res. 2020, 59, 9004−9014

of $KMnO_4$ oxidizer yielded GO with higher oxygen content and had more surface functional oxygen groups than GO produced without acid soaking. Prior literature concluded that the intercalation of sulfuric acid in graphite happens within minutes, but our results indicate that longer acid soaking time improves the degree of oxidation. Additionally, increasing the mixing speed during oxidation for acid-soaked parent materials decreases the degree of oxidation in the product GO. This is interesting because it is counterintuitive to the expectation that mixing improves the diffusion-controlled oxidation reaction. We hypothesized that improved mixing for acid-soaked runs is encouraging secondary reaction instead of the oxidation reaction.

The GO synthesized at oxidation temperatures of 10, 22, and 33 °C showed that heat of reaction increases with increasing reaction temperature. The elemental analysis showed less oxygen content in the final GO produced at lower temperatures. However, the XPS of C 1s and O 1s spectra of these GOs showed that the lower temperature synthesis has less sp^3 carbon and more carbon and oxygen bonds compared to the higher temperature synthesis. Similarly, lower temperature synthesis also gives more aromatic oxygen bonds compared to the higher temperature synthesis. Therefore, the amount of time graphite is soaked in acid before the addition of oxidizer and the reaction temperature have effects on the degree and type of oxygen content in the final GO.

Finally, the adiabatic temperature increase due to the heat of solution of $KMnO_4$ in acid and the heat of oxidation reaction is about 16 K. This temperature increase is large enough to reach the reported unstable temperature of Mn_2O_7 at 55 °C. However, the Mn_2O_7 produced in modified Hummers' method is in solution and dilute enough that it is not likely to be explosive at 55 °C, but the solution is sensitive to organic impurities and care should be taken to keep the reactants and reaction mixture free of organic impurities. Finally, in order to quench the oxidation reaction, the reaction mass is added to water. It should be noted that the acid−water reaction is highly exothermic and it could potentially cause hot spots and thermal runaway conditions in the absence of adequate mixing and cooling capacity.

■ ASSOCIATED CONTENT

Supporting Information

The Supporting Information is available free of charge at https://pubs.acs.org/doi/10.1021/acs.iecr.0c00644.

Details on RC1*e* equipment, characterization details, *Re*, and adiabatic temperature calculations (PDF)

■ AUTHOR INFORMATION

Corresponding Author

Micah J. Green − *Artie McFerrin Department of Chemical Engineering, Texas A&M University, College Station, Texas 77843, United States;* orcid.org/0000-0001-5691-0861; Phone: 979-862-1588; Email: micah.green@tamu.edu; Fax: 979-458-1493

Authors

Pritishma Lakhe − *Artie McFerrin Department of Chemical Engineering and Mary Kay O'Connor Process Safety Center, Texas A&M University, College Station, Texas 77843, United States*

Devon L. Kulhanek − *Artie McFerrin Department of Chemical Engineering, Texas A&M University, College Station, Texas 77843, United States*

Xiaofei Zhao − *Artie McFerrin Department of Chemical Engineering, Texas A&M University, College Station, Texas 77843, United States;* orcid.org/0000-0002-0593-8490

Maria I. Papadaki − *Department of Environmental and Natural Resources Management, School of Engineering, University of Patras, Agrinio 30100, Greece*

Mainak Majumder − *Nanoscale Science and Engineering Laboratory (NSEL), Department of Mechanical and Aerospace Engineering, Monash University, Clayton, Victoria 3168, Australia;* orcid.org/0000-0002-0194-9387

Complete contact information is available at: https://pubs.acs.org/10.1021/acs.iecr.0c00644

Notes

The authors declare no competing financial interest.

■ ACKNOWLEDGMENTS

The authors thank Dr. Wanmei Sun and Dr. Smit A. Shah for their valuable input and guidance. The funding was provided by the Mary Kay O'Connor Process Safety Center (MKOPSC) at Texas A&M University and the U.S. National Science Foundation (Grant CMMI-1760859).

■ REFERENCES

(1) Basu, J.; Basu, J. K.; Bhattacharyya, T. K. The evolution of graphene-based electronic devices. *Int. J. Smart Nano Mater.* **2010**, *1*, 201−223.

(2) Nima, Z. A.; Vang, K. B.; Nedosekin, D.; Kannarpady, G.; Saini, V.; Bourdo, S. E.; Majeed, W.; Watanabe, F.; Darrigues, E.; Alghazali, K. M.; Alawajji, R. A.; Petibone, D.; Ali, S.; Biris, A. R.; Casciano, D.; Ghosh, A.; Salamo, G.; Zharov, V.; Biris, A. S. Quantification of cellular associated graphene and induced surface receptor responses. *Nanoscale* **2019**, *11*, 932−944.

(3) Shi, G.; Araby, S.; Gibson, C. T.; Meng, Q.; Zhu, S.; Ma, J. Graphene platelets and their polymer composites: fabrication, structure, properties, and applications. *Adv. Funct. Mater.* **2018**, *28*, 1706705.

(4) Dreyer, D. R.; Bielawski, C. W. Carbocatalysis: Heterogeneous carbons finding utility in synthetic chemistry. *Chemical Science* **2011**, *2*, 1233−1240.

(5) Dreyer, D. R.; Todd, A. D.; Bielawski, C. W. Harnessing the chemistry of graphene oxide. *Chem. Soc. Rev.* **2014**, *43*, 5288−5301.

(6) Boukhvalov, D. W.; Dreyer, D. R.; Bielawski, C. W.; Son, Y.-W. A computational investigation of the catalytic properties of graphene oxide: Exploring mechanisms by using DFT methods. *ChemCatChem* **2012**, *4*, 1844−1849.

(7) Kauling, A. P.; Seefeldt, A. T.; Pisoni, D. P.; Pradeep, R. C.; Bentini, R.; Oliveira, R. V.; Novoselov, K. S.; Castro Neto, A. H. The Worldwide graphene flake production. *Adv. Mater.* **2018**, *30*, 1803784.

(8) Zurutuza, A.; Marinelli, C. Challenges and opportunities in graphene commercialization. *Nat. Nanotechnol.* **2014**, *9*, 730.

(9) Eigler, S.; Dotzer, C.; Hirsch, A. Visualization of defect densities in reduced graphene oxide. *Carbon* **2012**, *50*, 3666−3673.

(10) Marcano, D. C.; Kosynkin, D. V.; Berlin, J. M.; Sinitskii, A.; Sun, Z.; Slesarev, A.; Alemany, L. B.; Lu, W.; Tour, J. M. Improved synthesis of graphene oxide. *ACS Nano* **2010**, *4*, 4806−4814.

(11) Pei, S.; Cheng, H.-M. The reduction of graphene oxide. *Carbon* **2012**, *50*, 3210−3228.

(12) Dimiev, A. M.; Tour, J. M. Mechanism of graphene oxide formation. *ACS Nano* **2014**, *8*, 3060−3068.

(13) Morimoto, N.; Suzuki, H.; Takeuchi, Y.; Kawaguchi, S.; Kunisu, M.; Bielawski, C. W.; Nishina, Y. Real-Time, in Situ Monitoring of the

Oxidation of Graphite: Lessons Learned. *Chem. Mater.* **2017**, *29*, 2150−2156.
(14) Chen, J.; Yao, B.; Li, C.; Shi, G. An improved Hummers method for eco-friendly synthesis of graphene oxide. *Carbon* **2013**, *64*, 225−229.
(15) Brodie, B. C. XIII. On the atomic weight of graphite. *Philos. Trans. R. Soc. London* **1859**, *149*, 249−259.
(16) Hummers, W. S., Jr; Offeman, R. E. Preparation of graphitic oxide. *J. Am. Chem. Soc.* **1958**, *80*, 1339−1339.
(17) Staudenmaier, L. Verfahren zur darstellung der graphitsäure. *Ber. Dtsch. Chem. Ges.* **1898**, *31*, 1481−1487.
(18) Hofmann, U.; König, E. Untersuchungen über graphitoxyd. *Zeitschrift für anorganische und allgemeine Chemie* **1937**, *234*, 311−336.
(19) Lavin-Lopez, M. d. P.; Romero, A.; Garrido, J.; Sanchez-Silva, L.; Valverde, J. L. Influence of different improved hummers method modifications on the characteristics of graphite oxide in order to make a more easily scalable method. *Ind. Eng. Chem. Res.* **2016**, *55*, 12836−12847.
(20) Li, C.; Shi, Y.; Chen, X.; He, D.; Shen, L.; Bao, N. Controlled synthesis of graphite oxide: formation process, oxidation kinetics, and optimized conditions. *Chem. Eng. Sci.* **2018**, *176*, 319−328.
(21) Seiler, S.; Halbig, C. E.; Grote, F.; Rietsch, P.; Börrnert, F.; Kaiser, U.; Meyer, B.; Eigler, S. Effect of friction on oxidative graphite intercalation and high-quality graphene formation. *Nat. Commun.* **2018**, *9*, 836.
(22) Dreyer, D. R.; Park, S.; Bielawski, C. W.; Ruoff, R. S. The chemistry of graphene oxide. *Chem. Soc. Rev.* **2010**, *39*, 228−240.
(23) Lee, S.; Eom, S. H.; Chung, J. S.; Hur, S. H. Large-scale production of high-quality reduced graphene oxide. *Chem. Eng. J.* **2013**, *233*, 297−304.
(24) Simon, A.; Dronskowski, R.; Krebs, B.; Hettich, B. The crystal structure of Mn2O7. *Angew. Chem., Int. Ed. Engl.* **1987**, *26*, 139−140.
(25) Tölle, F. J.; Gamp, K.; Mülhaupt, R. Scale-up and purification of graphite oxide as intermediate for functionalized graphene. *Carbon* **2014**, *75*, 432−442.
(26) Justh, N.; Berke, B.; László, K.; Szilágyi, I. M. Thermal analysis of the improved Hummers' synthesis of graphene oxide. *J. Therm. Anal. Calorim.* **2018**, *131*, 2267−2272.
(27) Vryonis, O.; Andritsch, T.; Vaughan, A. S.; Lewin, P. L. Structural and chemical comparison between moderately oxygenated and edge oxygenated graphene: mechanical, electrical and thermal performance of the epoxy nanocomposites. *SN Appl. Sci.* **2019**, *1*, 1275.
(28) Fogler, H. S. *Essentials of Chemical Reaction Engineering*; Pearson Education: 2010.
(29) Kang, J. H.; Kim, T.; Choi, J.; Park, J.; Kim, Y. S.; Chang, M. S.; Jung, H.; Park, K. T.; Yang, S. J.; Park, C. R. Hidden second oxidation step of Hummers method. *Chem. Mater.* **2016**, *28*, 756−764.
(30) Park, J.; Kim, Y. S.; Sung, S. J.; Kim, T.; Park, C. R. Highly dispersible edge-selectively oxidized graphene with improved electrical performance. *Nanoscale* **2017**, *9*, 1699−1708.
(31) Römpp, H.; Falbe, J.; Amelingmeier, E. *Römpp kompakt Basislexikon Chemie: M-Re*; Thieme: 1999; Vol. 3.
(32) Morimoto, N.; Kubo, T.; Nishina, Y. Tailoring the oxygen content of graphite and reduced graphene oxide for specific applications. *Sci. Rep.* **2016**, *6*, 21715.
(33) Glemser, O.; Schröder, H. Über Manganoxyde. II. Zur Kenntnis des Mangan (VII)-oxyds. *Z. Anorg. Allg. Chem.* **1953**, *271*, 293−304.
(34) Lee, S.; Oh, J.; Ruoff, R. S.; Park, S. Residual acetone produces explosives during the production of graphite oxide. *Carbon* **2012**, *50*, 1442−1444.

https://dx.doi.org/10.1021/acs.iecr.0c00644
Ind. Eng. Chem. Res. 2020, 59, 9004−9014